

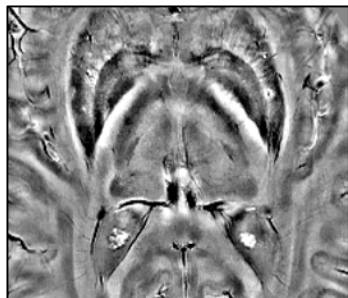
# QSM standardisation routine for unbiased whole-brain analysis

Julio Acosta-Cabronero<sup>1</sup>, Matthew TJ Betts<sup>1</sup>, Arturo Cardenas-Blanco<sup>1</sup>, Shan Yang<sup>2</sup>, Oliver Speck<sup>2</sup>, and Peter J Nestor<sup>1</sup>

<sup>1</sup>German Center for Neurodegenerative Diseases (DZNE), Magdeburg, Saxony-Anhalt, Germany, <sup>2</sup>Biomedical Magnetic Resonance (BMMR), Otto-von-Guericke University, Magdeburg, Saxony-Anhalt, Germany

**Target Audience.** Researchers with interest in quantitative susceptibility mapping (QSM).

**Purpose.** The development of an unbiased processing pipeline to enable voxel-/cluster-wise QSM analysis.



**Introduction.** Recent proof-of-concept studies have confirmed QSM's strong potential to yield new insights in degenerative brain diseases (Acosta-Cabronero et al., Plos One 2013; Langkammer et al., Radiology 2013). Most studies to date have demonstrated susceptibility alterations in deep brain nuclei by way of ROI analyses in entire subcortical structures. Undoubtedly, however, deep grey matter's biochemistry is spatially heterogeneous (see large greyscale variations in high resolution 7T QSM illustration), as it would be expected by the wide range of functional activities these deep brain centres are thought to be involved in. Additionally, in neurodegenerative diseases, focal micro-vascular lesions or calcifications can dominate regional QSM measurements due to their high hemosiderin/methaemoglobin (highly paramagnetic) or alkaline salt (highly diamagnetic) content, respectively. If inferences (e.g. about the QSM relationship with ageing or disease) are being made on the hypothesis that QSM effects are driven by storage iron or more generically, by non-heme metals, it would be desirable to demonstrate such claim with the study of the spatial extent, in addition to strength, of QSM alterations. In order to enable whole-brain statistical analysis at the voxel or cluster level, the present abstract introduces a processing pipeline for standardising susceptibility-weighted data and demonstrates its stability on a 7 Tesla MRI dataset.

**Methods.** *Subjects.* N=16 healthy volunteers (age: 22-29 yrs.) were recruited. *SWI.* MRI experiments were performed on a Siemens MAGNETOM 7T system with a standard 32-channel head-coil for reception. Whole-brain 7T SWI consisted of a 3D GRE sequence with four monopolar readouts (BW=300 Hz/px each) per (slab-selective) excitation. Note that only the first echo was fully flow compensated. Other imaging parameters were: TR/TE/ $\alpha$ =28ms/8,13,18,23ms/12°; matrix 320x320; 88 axial slices; voxel size 0.8x0.8x1.6 mm<sup>3</sup> with 7/8 phase and slice k-space undersampling; total scan time was 10:05 minutes. The obvious advantage of this multi-echo approach is that in addition to QSM, it also enables R2\* mapping (not shown here), with the inconvenience, however, that flow effects are more apparent than in fully flow compensated acquisitions and the point spread function for multi-echo combined data tends to be wider. *Data processing.* Sum-of-squares and Siemens (syngo VB17/19) adaptive combination generated undesirable singular-phase errors; thus, multi-channel complex data were combined for optimal phase reconstruction using a previously proposed adaptive method (Yang et al. ISMRM 2009). In order to further reduce potential phase errors in the combination of multi-echo data, we estimated the off-resonance frequency from the complex GRE signal evolution by formulating a noise-weighted, nonlinear least-squares fitting problem (Liu et al., MRM 2013). Phases were subsequently unwrapped with a direct Laplacian method (Schofield & Zhu, Opt Lett 2003). Then, locally sourced inductions (i.e. foreground field shifts) were revealed through background field extraction with the PDF algorithm (Liu et al. NMR Biomed 2011, available at: <http://weill.cornell.edu/mri/pages/qsm.html>). Note that BET2 (f=0.2) for brain-mask estimation and large zero-padding were needed for optimal PDF. This was followed by spherical mean value post-filtering (sphere radius of 4 mm) to further remove background field residuals (Li & Leigh, JMR 2001). Then, for conditioning the susceptibility restoration problem, the iterative, morphology-enabled, non-linear dipole inversion (MEDIN) solver with dynamic noise-weighting reduction (MERIT) was used (Liu et al., MRM 2013, available at: <http://weill.cornell.edu/mri/pages/qsm.html>). MEDIN incorporates a total-variation operation to optimally "compartmentalise" (aided by magnitude gradient information) an otherwise data-consistent solution. The regularisation parameter was chosen so that the consistency-term residual matched an estimated phase-noise level. Note that data-consistency terms (both in PDF & MEDIN formulations) were weighted by an estimated SNR map to compensate for magnitude-dependent phase noise variations. Regularised solutions were finally normalised (by direct subtraction) to the QSM median value in a largely homogeneous (low group dispersion) posterior parietal white matter region. Note also that normalisation region selection is an area of active research – manual selection is far from desirable in this context but automated methods are yet to be proposed and cross-validated. *Spatial standardisation.* RF-bias corrected (N4-ITK; Tustison et al., IEEE TMI 2010) SNR maps for each dataset were standardised (to a study-wise space) by way of a parallel routine for template creation based on ANTSv1.9's diffeomorphic Greedy-SyN

transformation model (Avants et al., Med Image Anal 2008). Simultaneous co-registrations were driven by a cross-correlation minimisation performed over three resolutions with a maximum of 90 iterations at the coarsest level, 30 at the next coarsest and 90 at full resolution; template update step size was set to 0.1. Six full runs of the above multi-resolution routine were carried out to ensure stable convergence. QSM spatial standardisation was achieved by application of the resulting transformation fields followed by trilinear resampling. In order to qualitatively assess the validity of the proposed approach, normalised QSM volumes were averaged and a data dispersion map was calculated.

**Results.** Group-average (mean) and standard deviation (sigma) QSM distributions reflected good agreement across normalised maps (see illustrative panels on the left). It is noteworthy that QSM measurements in deep grey matter and white matter tissue are more stable (i.e. greater absolute value and lower variance) than those in misregistration-prone cortical areas.

**Discussion.** QSM group comparisons at a voxel (or data-driven cluster) level require stable dipole inversions and accurate co-registration methodologies. The present abstract proposes a processing pipeline that demonstrates robust performance with 7 Tesla MRI data.

**Conclusion.** Regional QSM measurements typically target entire subcortical structures (for assessing methods performance or in clinical applications), but clearly, magnetic susceptibility sources e.g. across the basal ganglia and thalamus are locally heterogeneous; this illustrates that enabling whole-brain unbiased local inferences would be desirable. The corollary of this work is that such analysis can be performed with relative confidence.

